

Investigating the Edge of Stability Phenomenon in Reinforcement Learning

Rares Iordan

University College London, United Kingdom

RARES-IOAN.IORDAN.18@UCL.AC.UK

Marc Peter Deisenroth

University College London, United Kingdom

M.DEISENROTH@UCL.AC.UK

Mihaela Rosca

University College London, United Kingdom*

MIHAELA.ROSCA.19@UCL.AC.UK

Abstract

Recent progress has been made in understanding optimisation dynamics in neural networks trained with full-batch gradient descent with momentum with the uncovering of the edge of stability phenomenon in supervised learning [7]. The edge of stability phenomenon occurs as the leading eigenvalue of the Hessian reaches the divergence threshold of the underlying optimisation algorithm for a quadratic loss, after which it starts oscillating around the threshold, and the loss starts to exhibit local instability but decreases over long time frames. In this work, we explore the edge of stability phenomenon in reinforcement learning (RL), specifically off-policy Q-learning algorithms across a variety of data regimes, from offline to online RL. Our experiments reveal that, despite significant differences to supervised learning, such as non-stationarity of the data distribution and the use of bootstrapping, the edge of stability phenomenon can be present in off-policy deep RL. Unlike supervised learning, however, we observe strong differences depending on the underlying loss, with DQN — using a Huber loss — showing a strong edge of stability effect that we do not observe with C51 — using a cross entropy loss. Our results suggest that, while neural network structure can lead to optimisation dynamics that transfer between problem domains, certain aspects of deep RL optimisation can differentiate it from domains such as supervised learning.

1. The Edge of Stability Phenomenon

Cohen et al. [7] use a thorough experimental study to shed light on deep learning optimisation dynamics by showing that full-batch gradient descent training in supervised learning exhibits two phases: *progressive sharpening* and *edge of stability*. In the first stage of training, *progressive sharpening*, the leading eigenvalue of the Hessian, λ_1 , increases steadily and the loss decreases monotonically. As λ_1 increases, it reaches the divergence threshold of the underlying optimisation algorithm under a quadratic loss assumption (we will call this “the quadratic divergence threshold”); for gradient descent with learning rate η and momentum decay rate β , the quadratic divergence threshold is $\frac{1}{\eta}(2 + 2\beta)$. As λ_1 reaches the quadratic divergence threshold, *the edge of stability phenomenon* occurs: the loss starts to exhibit short-term instabilities, while decreasing over long time scales; λ_1 no longer steadily increases, but fluctuates around the threshold. For cross entropy losses, the edge of stability area is followed by a decrease in λ_1 , while for mean squared error losses

* Also at Google Deepmind.

λ_1 stays in the edge of stability area. Similar results are shown for stochastic gradient descent, across batch sizes, though the effect is less pronounced as the batch sizes decrease [7].

The edge of stability phenomenon shows that neural network training is strongly affected by the quadratic divergence threshold of the underlying optimisation algorithm, and exceeding it leads to training instabilities. This observation has garnered a lot of interest, with recent works having analysed the edge of stability phenomenon in supervised learning with both theoretical and empirical tools [2, 6, 9, 21, 26]. To the best of our knowledge, no studies on the edge of stability phenomenon have been made outside of supervised learning. We complement this body of work by empirically investigating whether the edge of stability phenomenon occurs in off-policy deep RL algorithms DQN and C51 across a variety of data regimes, from offline to online learning. Upon acceptance, we will make the code and data used publicly available.

2. Challenges with optimisation in off-policy deep reinforcement learning

To investigate whether the edge of stability phenomenon translates to deep RL, we conduct experiments using DQN [23] and C51 [3], two off-policy algorithms that model the state-action value function $Q(s, a; \theta)$ with a neural network with parameters θ . We study both DQN and C51 as their losses correspond to the mean squared error and cross entropy loss used in supervised learning, studied by Cohen et al. [7] when investigating the edge of stability phenomenon. For DQN, we investigate the more commonly used the Huber loss, which is quadratic around 0:

$$\min_{\theta} E(\theta) = \begin{cases} \mathbb{E}_{(s,a,s',r) \sim \mathcal{R}} \frac{1}{2} \left(Q(s, a; \theta) - \left(r + \gamma \max_{a'} Q(s', a'; \theta) \right) \right)^2, & \text{if } (\cdot)^2 \leq 1 \\ \mathbb{E}_{(s,a,s',r) \sim \mathcal{R}} \left| Q(s, a; \theta) - \left(r + \gamma \max_{a'} Q(s', a'; \theta) \right) \right| - \frac{1}{2}, & \text{otherwise.} \end{cases} \quad (1)$$

C51 [3], the distributional counterpart of DQN, uses distributional quantiles instead of operating in expectation as in Eq (1), leading to a cross entropy loss; for details, we refer to Appendix B.2.

Off-policy deep RL algorithms like DQN and C51 differ from supervised learning both through their objectives—which use bootstrapping—and the data present in the replay buffer \mathcal{R} used for learning the agent, which can be non-stationary, have noise inserted to help exploration, and can be obtained from the agent’s own experience. All the above affect optimisation dynamics in deep RL, and have been studied individually [1, 10, 13, 23, 25]. Bootstrapping — the dependence of the regression target in Eq (1) on the Q-function — can lead to increased variance and bias in model updates [22, 27]. To mitigate instabilities introduced by bootstrapping often a target network is used, where old parameters updated at regular intervals are used to construct the target instead of the current parameters; both DQN and C51 use target networks. In online RL, where the replay buffer \mathcal{R} is filled with the agent’s own experience, the non-stationarity of the data present in the replay buffer \mathcal{R} violates the i.i.d. assumption required by many optimisation algorithms and gradient updates might not form a gradient vector field [4]. Offline RL [11, 12, 16], where the agent learns from a fixed replay buffer often gathered from another agent or expert demonstrations, can mitigate some of the training challenges with online RL, but can suffer from poor agent performance due to distributional shift [19] — the discrepancy between the data distribution used for learning, present in the offline dataset (the replay buffer), and the distribution the policy encounters during execution.

Given these peculiarities of RL, it is unclear how optimisation effects observed in supervised learning, such as the edge of stability results, transfer to deep RL, and they interact with the be-

behaviour of the loss function. Since the value of the loss function in RL has not been connected with agent performance, many RL works do not study or report loss function behaviour, and focus on the agent reward instead. Here, we focus on the behaviour of the loss function in deep RL and aim to connect it with the value of the leading Hessian eigenvalue through edge of stability results.

3. Investigating the edge of stability in phenomenon reinforcement learning

When studying the edge of stability phenomenon in deep RL, we aim to isolate the effect of the data distribution from the other aspects of RL, such as the use of bootstrapping. We thus train agents across multiple data regimes, ranging from offline learning to online learning. We use gradient descent with and without momentum on MinAtar [28], a subset of Atari games with reduced visual complexity; MinAtar results have been shown to translate to Atari [5]. We show results on Breakout in the main text, with Space Invaders results in Appendix A.4. Since not all the data regimes we consider allow for full-batch training, results in this section use mini-batch training; we provide full-batch training results in Appendix A.2. Experimental details are provided in Appendix B.4, and training details of the pre-trained agent used in the offline RL experiments are in Appendix B.3.

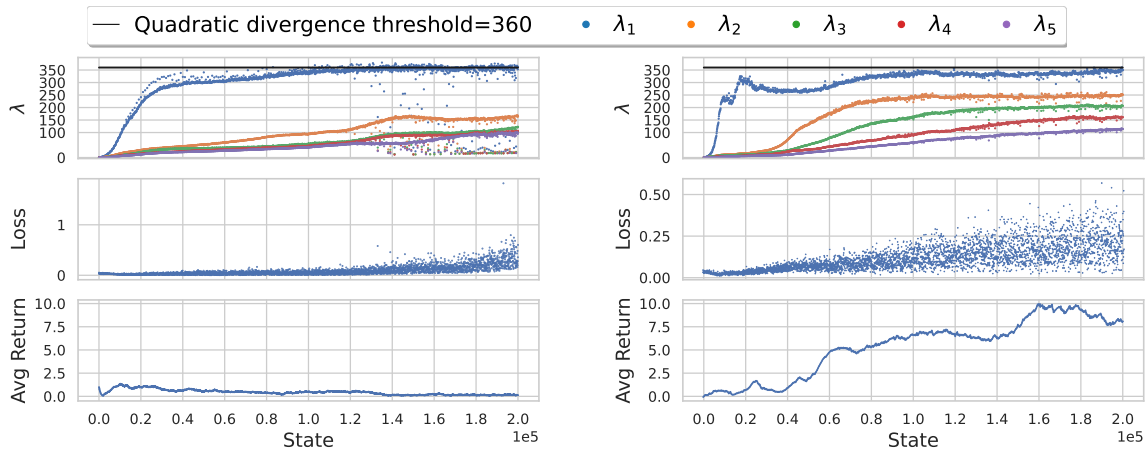
3.1. DQN

Offline RL: agent trained using experience generated from a greedy pre-trained policy. We use a pre-trained agent’s greedy policy to generate a replay buffer of 10^6 transitions and use this to train a new DQN agent. This setup is closest to that of supervised learning, and isolates the effect of the RL losses and bootstrapping from RL specific effects on the data distribution. Figure 1a shows a clear edge of stability effect: the leading eigenvalue λ_1 grows until reaching the quadratic divergence threshold, after which fluctuates around it and the loss function shows increasing instabilities; this is consistent with results using the mean squared error in supervised learning. Consistent with existing results [12], the performance of the agent is poor, likely due distributional shift.

Offline RL: agent trained using experience generated from an ϵ -greedy pre-trained policy. To address the challenges with distributional shift and increase the diversity of agent experience, instead using greedy actions taken by the pre-trained agent to generate the replay buffer, we use an ϵ -greedy policy with 0.7 probability of taking greedy action from the pre-trained agent and 0.3 probability of a random action. This is akin to the concurrent setting in Fujimoto et al. [12]. Results in Figure 1b show that this intervention vastly improves the reward obtained by the agent compared to the previous setting explored, but optimisation dynamics retain the edge of stability behaviour.

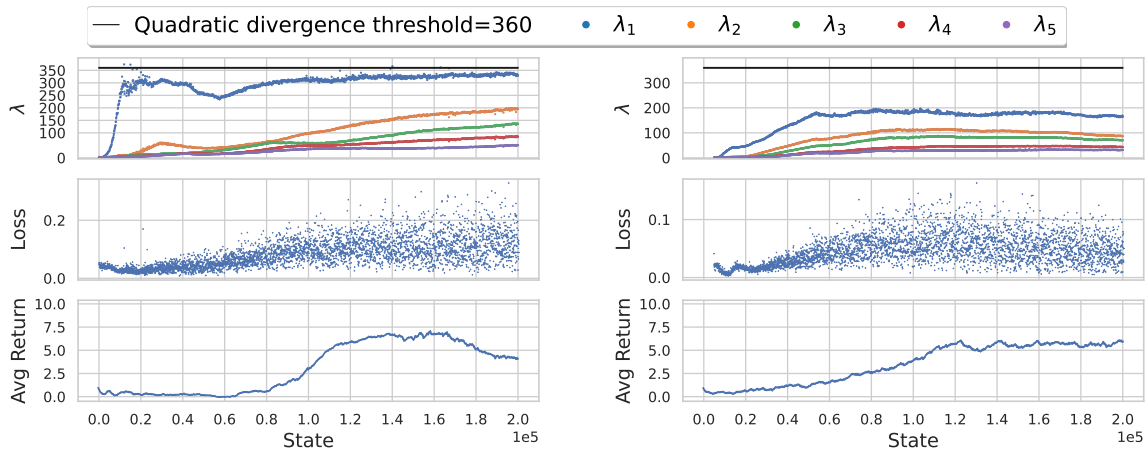
Offline RL: agent trained from the replay buffer of a pre-trained agent. We train an agent using the last 10^6 transitions obtained from the pre-trained agent’s online phase; this is known as the final buffer setting [1, 12]. This brings us closer to online RL: we still use a fixed replay buffer to train the agent, but that dataset contains transitions from a changing distribution. This allows us to isolate the effect of the replay buffer being obtained from a series of changing policies from the interactions of the agent’s behaviour affecting its own replay buffer, as we see in online learning. Results in Figure 1c show that here too, we observe the edge of stability phenomenon.

Online RL: agent trained from a replay buffer of its own experience. In online RL, the replay buffer is obtained from the agent’s own experience, leading to the related challenges mentioned in Section 2. Figure 1d shows that the leading eigenvalues of the Hessian grow early in training but plateau below the quadratic divergence threshold; despite λ_1 not reaching the quadratic divergence threshold, once it plateaus we observe increased instability in the loss function.



(a) Offline RL: agent trained using experience generated from a greedy pre-trained policy.

(b) Offline RL: agent trained using experience generated from an ϵ -greedy pre-trained policy.

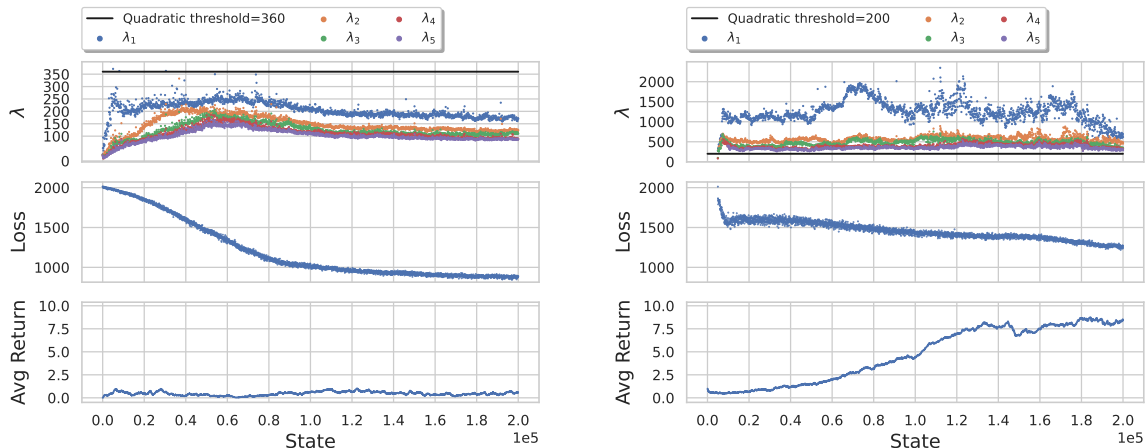


(c) Offline RL: agent trained from the replay buffer of a pre-trained agent.

(d) Online RL: agent trained from a replay buffer of its own experience.

Figure 1: **DQN**. The edge of stability phenomenon is observed in the offline setting (1a, 1b, 1c): the leading eigenvalue λ_1 rises to the quadratic divergence threshold induced by the underlying optimisation algorithm, after which it fluctuates around the threshold; when λ_1 reaches the quadratic divergence threshold, we observe more loss instability, but this does not always get reflected in the agent’s reward. In online training, λ_1 does not reach the quadratic divergence threshold and we do not observe the edge of stability phenomenon, though λ_1 plateaus early in training.

We show full-batch results across the above offline RL cases above in Figures 5, 7, 9 in the Appendix, which consistently show that as λ_1 fluctuates around the quadratic divergence threshold the loss function exhibits increased instabilities. We note that while changing the target network can have a short term effect on λ_1 , it does not drastically affect it’s long term trajectory and the edge of stability phenomenon.



(a) Offline RL: agent trained using experience generated from a greedy pre-trained policy.

(b) Online RL: agent trained from a replay buffer of its own experience.

Figure 2: **C51**. When using C51 in an offline setting, we notice that the leading eigenvalue λ_1 does not always reach the edge of stability threshold. In online learning, we observe that λ_1 greatly exceeds the quadratic divergence threshold. Like in supervised learning, however, using a cross entropy loss leads to a decrease of λ_1 later in training.

3.2. C51

When investigating the edge of stability effect using C51 across all the above data regimes, we observe that C51 does not clearly exhibit the edge of stability behaviour; we show selected results in Figure 2 and additional results in Figures 3 and 11 in the Appendix. However, similar to the observations in supervised learning with cross-entropy loss [7], we notice that λ_1 grows early in training, after which it consistently decreases. In offline learning (Figure 2a), the leading eigenvalue λ_1 , usually stays under the quadratic divergence threshold, but this is not the case in online learning (Figure 2b), where λ_1 is consistently significantly above the quadratic divergence threshold. This observation might explain why we observed increased challenges with training C51 in this setting compared to DQN (results in Figure 2b use stochastic gradient descent without momentum, as using momentum led to very poor results, see Figure 3d in the Appendix).

4. Discussion

We examined the edge of stability effect in DQN and C51, two off-policy deep RL algorithms on simple environments. Our findings suggest that *the edge of stability phenomenon can be induced by neural network optimisation in deep RL, but whether this occurs depends on underlying algorithm*. We observed that DQN exhibits the edge of stability behaviour in offline RL, with a diminished effect in online RL. In contrast, we did not observe a consistent edge of stability effect when using C51, but nonetheless did observe a connection between large leading Hessian eigenvalues and challenges in training C51 agents.

Caveats and future work. Our results were obtained on the MinAtar environment; we hope that future studies will expand our results to a wider range of environments. Following Cohen

et al. [7], we investigate the edge of stability phenomenon in RL when using gradient descent with momentum; we believe future work can expand our exploration to adaptive optimisers commonly used in RL, such as Adam [18], as has recently been done in supervised learning [8]. We further hope future research can connect the leading eigenvalue of the Hessian to the agent's performance, not only the loss, as has been done in supervised learning with generalisation [14, 15, 17, 20].

References

- [1] Rishabh Agarwal, Dale Schuurmans, and Mohammad Norouzi. Striving for simplicity in off-policy deep reinforcement learning. *CoRR*, abs/1907.04543, 2019. URL <http://arxiv.org/abs/1907.04543>.
- [2] Kwangjun Ahn, Jingzhao Zhang, and Suvrit Sra. Understanding the unstable convergence of gradient descent, 2022.
- [3] Marc G. Bellemare, Will Dabney, and Rémi Munos. A distributional perspective on reinforcement learning. *CoRR*, abs/1707.06887, 2017. URL <http://arxiv.org/abs/1707.06887>.
- [4] Emmanuel Bengio, Joelle Pineau, and Doina Precup. Interference and generalization in temporal difference learning. In Hal Daumé III and Aarti Singh, editors, *Proceedings of the 37th International Conference on Machine Learning*, volume 119 of *Proceedings of Machine Learning Research*, pages 767–777. PMLR, 13–18 Jul 2020. URL <https://proceedings.mlr.press/v119/bengio20a.html>.
- [5] Johan Samir Obando Ceron and Pablo Samuel Castro. Revisiting rainbow: Promoting more insightful and inclusive deep reinforcement learning research. In *International Conference on Machine Learning*, pages 1373–1383. PMLR, 2021.
- [6] Lei Chen and Joan Bruna. On gradient descent convergence beyond the edge of stability, 2022.
- [7] Jeremy M. Cohen, Simran Kaur, Yuanzhi Li, J. Zico Kolter, and Ameet Talwalkar. Gradient descent on neural networks typically occurs at the edge of stability. *CoRR*, abs/2103.00065, 2021. URL <https://arxiv.org/abs/2103.00065>.
- [8] Jeremy M Cohen, Behrooz Ghorbani, Shankar Krishnan, Naman Agarwal, Sourabh Medapati, Michal Badura, Daniel Suo, David Cardoze, Zachary Nado, George E Dahl, et al. Adaptive gradient methods at the edge of stability. *arXiv preprint arXiv:2207.14484*, 2022.
- [9] Alex Damian, Eshaan Nichani, and Jason D Lee. Self-stabilization: The implicit bias of gradient descent at the edge of stability. *arXiv preprint arXiv:2209.15594*, 2022.
- [10] Meire Fortunato, Mohammad Gheshlaghi Azar, Bilal Piot, Jacob Menick, Ian Osband, Alex Graves, Vlad Mnih, Rémi Munos, Demis Hassabis, Olivier Pietquin, Charles Blundell, and Shane Legg. Noisy networks for exploration. *CoRR*, abs/1706.10295, 2017. URL <http://arxiv.org/abs/1706.10295>.
- [11] Justin Fu, Aviral Kumar, Ofir Nachum, George Tucker, and Sergey Levine. D4RL: datasets for deep data-driven reinforcement learning. *CoRR*, abs/2004.07219, 2020. URL <https://arxiv.org/abs/2004.07219>.
- [12] Scott Fujimoto, David Meger, and Doina Precup. Off-policy deep reinforcement learning without exploration. *CoRR*, abs/1812.02900, 2018. URL <http://arxiv.org/abs/1812.02900>.

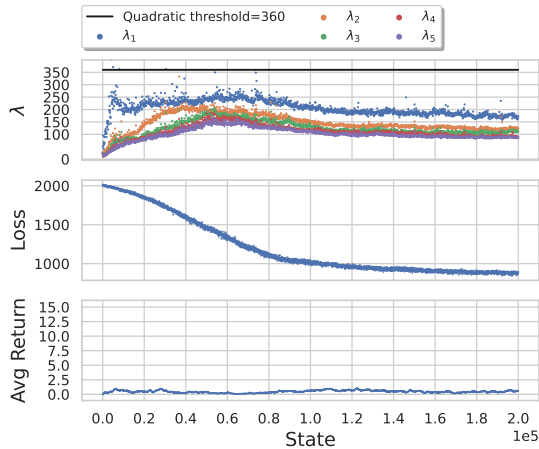
- [13] Scott Fujimoto, Herke van Hoof, and David Meger. Addressing function approximation error in actor-critic methods. *CoRR*, abs/1802.09477, 2018. URL <http://arxiv.org/abs/1802.09477>.
- [14] Sepp Hochreiter and Jürgen Schmidhuber. Flat minima. *Neural computation*, 9(1):1–42, 1997.
- [15] Stanisław Jastrzebski, Zachary Kenton, Nicolas Ballas, Asja Fischer, Yoshua Bengio, and Amos Storkey. On the relation between the sharpest directions of dnn loss and the sgd step length. In *International Conference on Learning Representations*.
- [16] Nathan Kallus and Masatoshi Uehara. Efficient evaluation of natural stochastic policies in offline reinforcement learning. *CoRR*, abs/2006.03886, 2020. URL <https://arxiv.org/abs/2006.03886>.
- [17] Nitish Shirish Keskar, Dheevatsa Mudigere, Jorge Nocedal, Mikhail Smelyanskiy, and Ping Tak Peter Tang. On large-batch training for deep learning: Generalization gap and sharp minima. In *International Conference on Learning Representations*.
- [18] Diederik P Kingma and Jimmy Ba. Adam: A method for stochastic optimization. *arXiv preprint arXiv:1412.6980*, 2014.
- [19] Sergey Levine, Aviral Kumar, George Tucker, and Justin Fu. Offline reinforcement learning: Tutorial, review, and perspectives on open problems. *CoRR*, abs/2005.01643, 2020. URL <https://arxiv.org/abs/2005.01643>.
- [20] Aitor Lewkowycz, Yasaman Bahri, Ethan Dyer, Jascha Sohl-Dickstein, and Guy Gur-Ari. The large learning rate phase of deep learning: the catapult mechanism. *arXiv preprint arXiv:2003.02218*, 2020.
- [21] Chao Ma, Daniel Kunin, Lei Wu, and Lexing Ying. Beyond the quadratic approximation: the multiscale structure of neural network loss landscapes, 2022.
- [22] Hamid Reza Maei. *Gradient Temporal-Difference Learning Algorithms*. PhD thesis, University of Alberta, CAN, 2011. AAINR89455.
- [23] Volodymyr Mnih, Koray Kavukcuoglu, David Silver, Alex Graves, Ioannis Antonoglou, Daan Wierstra, and Martin A. Riedmiller. Playing atari with deep reinforcement learning. *CoRR*, abs/1312.5602, 2013. URL <http://arxiv.org/abs/1312.5602>.
- [24] Volodymyr Mnih, Koray Kavukcuoglu, David Silver, Andrei A. Rusu, Joel Veness, Marc G. Bellemare, Alex Graves, Martin Riedmiller, Andreas K. Fidjeland, Georg Ostrovski, Stig Petersen, Charles Beattie, Amir Sadik, Ioannis Antonoglou, Helen King, Dharmarajan, Daan Wierstra, Shane Legg, and Demis Hassabis. Human-level control through deep reinforcement learning. *Nature*, 518(7540):529–533, 02 2015. ISSN 00280836. URL <http://dx.doi.org/10.1038/nature14236>.
- [25] Ashvin Nair, Bob McGrew, Marcin Andrychowicz, Wojciech Zaremba, and Pieter Abbeel. Overcoming exploration in reinforcement learning with demonstrations. *CoRR*, abs/1709.10089, 2017. URL <http://arxiv.org/abs/1709.10089>.

- [26] Mihaela Rosca, Yan Wu, Chongli Qin, and Benoit Dherin. On a continuous time model of gradient descent dynamics and instability in deep learning, 2023.
- [27] Tom Schaul, John Quan, Ioannis Antonoglou, and David Silver. Prioritized experience replay, 2016.
- [28] Kenny Young and Tian Tian. Minatar: An atari-inspired testbed for more efficient reinforcement learning experiments. *CoRR*, abs/1903.03176, 2019. URL <http://arxiv.org/abs/1903.03176>.

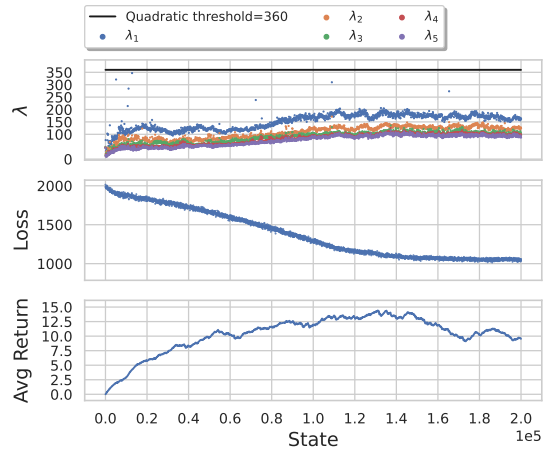
Appendix A. Additional experimental results

A.1. SGD with momentum results for C51 on Breakout

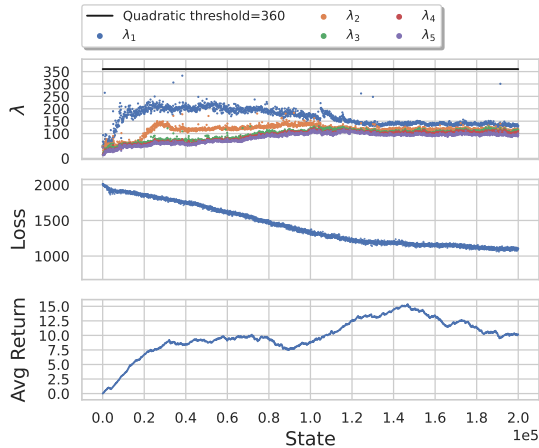
In Figure 3 we present C51 results on Breakout which do not clearly show an edge of stability effect. In the online regime, the eigenvalues consistently rise orders of magnitude above the quadratic threshold but reach low levels and plateau later in training.



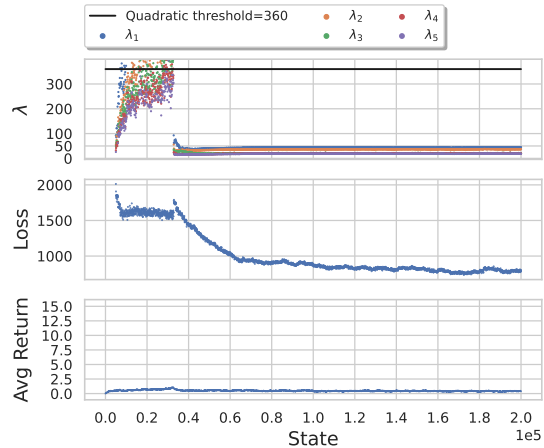
(a) Offline RL: agent trained using experience generated from a greedy pre-trained policy.



(b) Offline RL: agent trained using experience generated from an ϵ -greedy pre-trained policy.



(c) Offline RL: agent trained from the replay buffer of a pre-trained agent.



(d) Online RL: agent trained from a replay buffer of its own experience.

Figure 3: **C51**. When using C51 in an offline setting, we notice that the leading eigenvalue λ_1 does not always reach the edge of stability threshold. In online learning, we observe that λ_1 greatly exceeds the quadratic divergence threshold at the beginning of training after which it loses orders of magnitude and plateaus at a level below the quadratic threshold. Like in supervised learning, however, using a cross entropy loss leads to a decrease of λ_1 later in training.

A.2. Experiments on Breakout using SGD with momentum and full-batch

In Figure 4 we present full-batch experiments for DQN and C51 in the setting Offline RL: agent trained using experience generated from a greedy pre-trained policy, with a zoom in on the first time the quadratic threshold is achieved in Figure 5. DQN shows a clear edge of stability effect which is broken later during training where we see increased instabilities. C51 does not show an edge of stability effect with the eigenvalues plateauing over time.

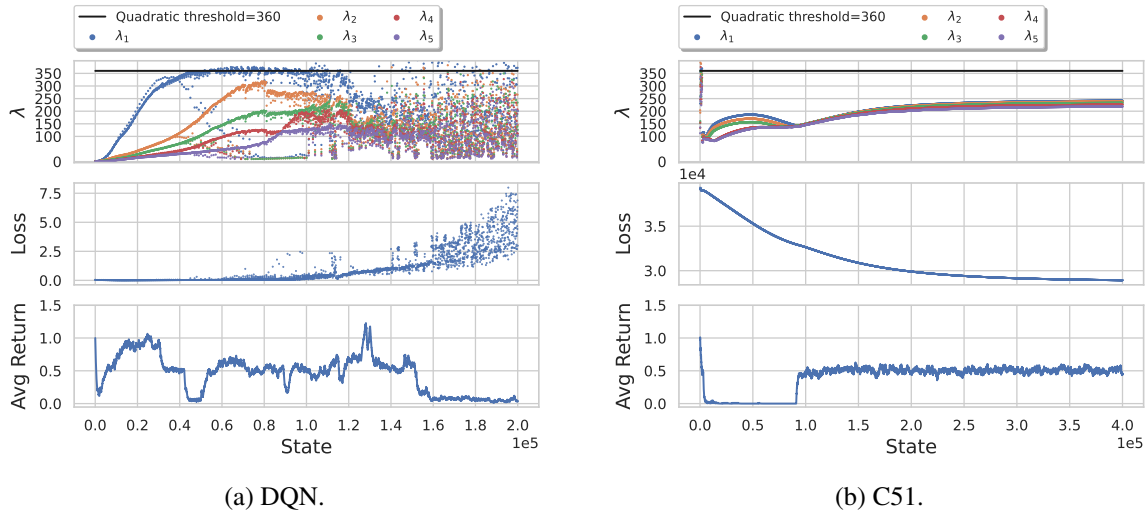


Figure 4: Full batch results in the setting Offline RL: agent trained using experience generated from a greedy pre-trained policy. **DQN** shows a strong edge of stability effect followed by instabilities in the eigenvalues. **C51** presents a rise and fall trend initially but over time the eigenvalues plateau.

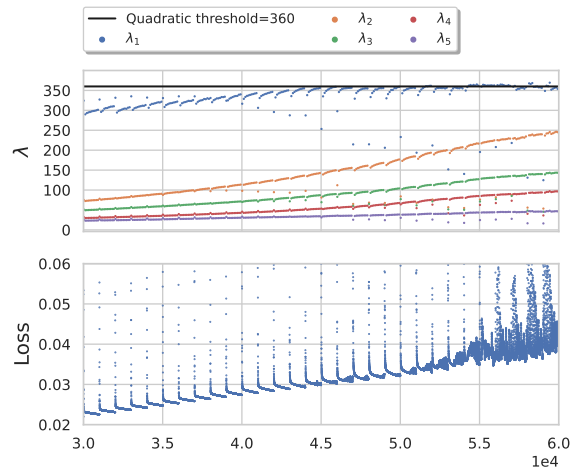


Figure 5: Zoom in full-batch results in the setting Offline RL: agent trained using experience generated from a greedy pre-trained policy. **DQN** shows a strong edge of stability effect. The behaviour is consistent with supervised learning where the loss and leading eigenvalue have the same relationship across changes to the target network.

In Figure 6 we present full-batch experiments for DQN and C51 in the setting Offline RL: agent trained using experience generated from an ϵ -greedy pre-trained policy, with a zoom in on the first time the quadratic threshold is achieved in Figure 7. Similar to the previous setting, DQN shows a clear edge of stability effect which is broken later during training where we see increased instabilities. C51 does not show an edge of stability effect with the eigenvalues plateauing over time.

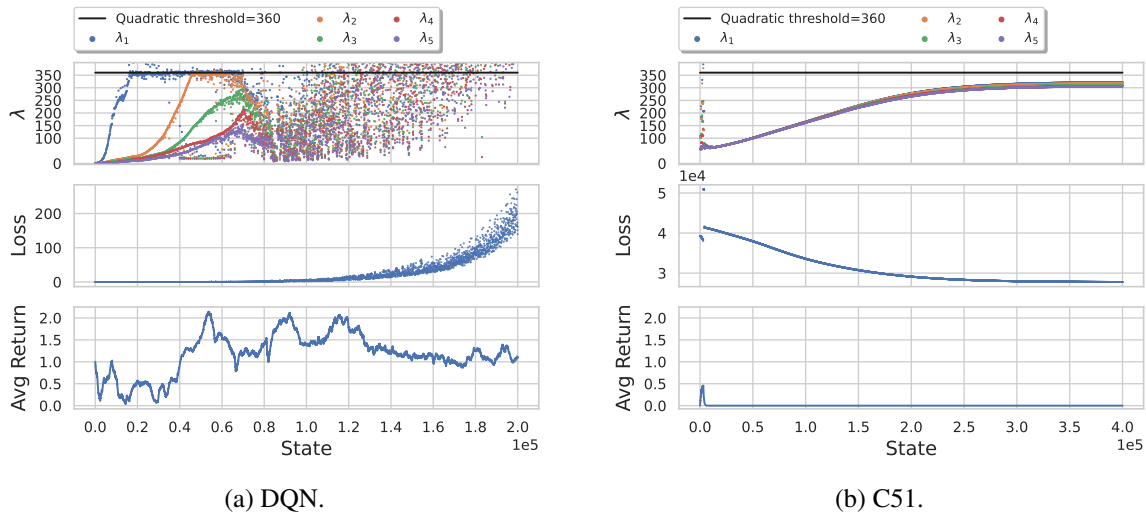


Figure 6: Full batch results in the setting Offline RL: agent trained using experience generated from an ϵ -greedy pre-trained policy. **DQN** shows a strong edge of stability effect followed by instabilities in the eigenvalues. In the case of **C51** the eigenvalues plateau over time.

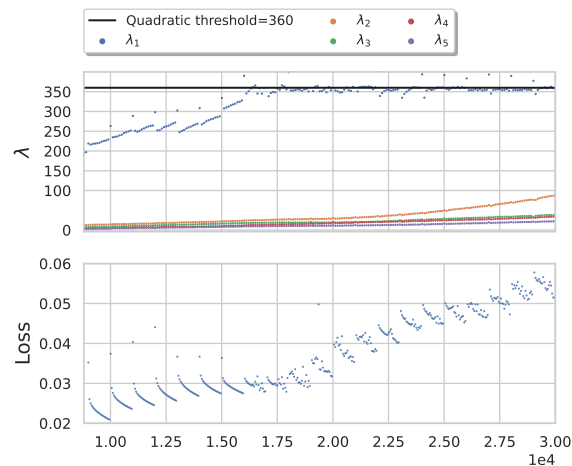


Figure 7: Zoom in full-batch results in the setting Offline RL: agent trained using experience generated from an ϵ -greedy pre-trained policy. **DQN** shows a strong edge of stability effect. The behaviour is consistent with supervised learning where the loss and leading eigenvalue have the same relationship across changes to the target network.

In Figure 8 we present full-batch experiments for DQN and C51 in the setting Offline RL: agent trained from the replay buffer of a pre-trained agent, with a zoom in on the first time the quadratic threshold is achieved in Figure 9. Similar to the previous two settings, DQN shows a clear edge of stability effect which is broken later during training where we see increased instabilities. C51 does not show an edge of stability effect with the eigenvalues plateauing over time.

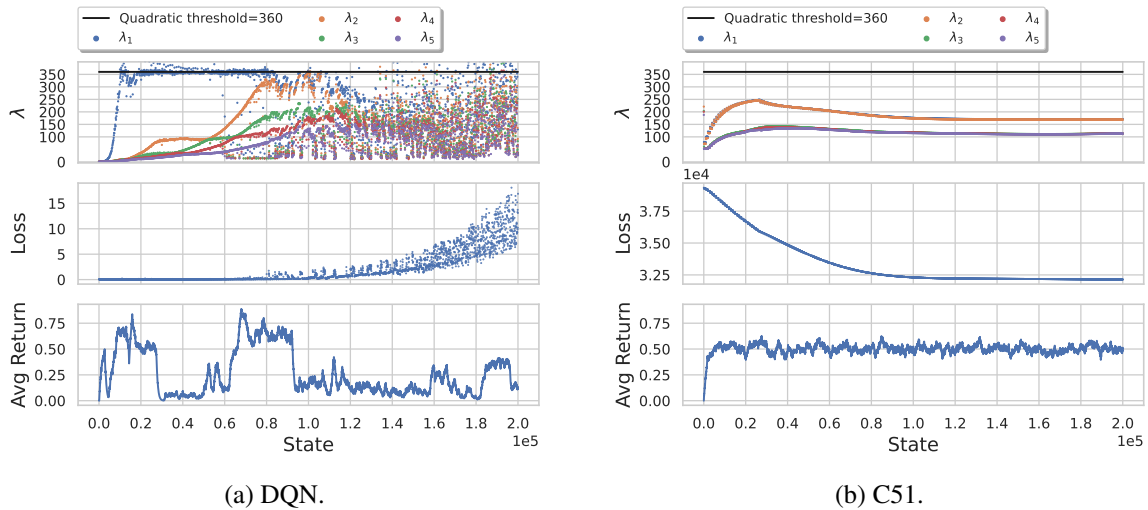


Figure 8: Full batch results in the setting Offline RL: agent trained from the replay buffer of a pre-trained agent. **DQN** shows a strong edge of stability effect. The behaviour is consistent with supervised learning where the loss and leading eigenvalue have the same relationship across changes to the target network.

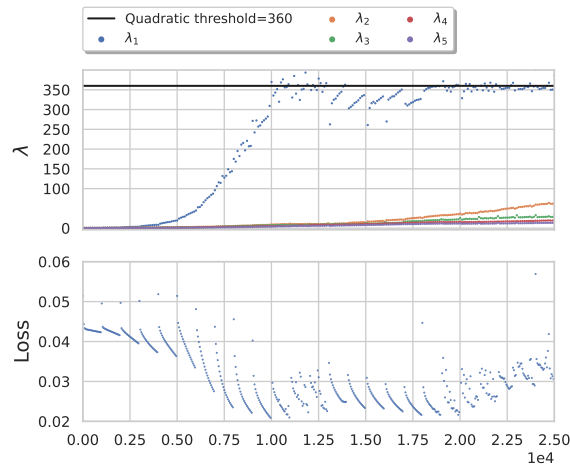
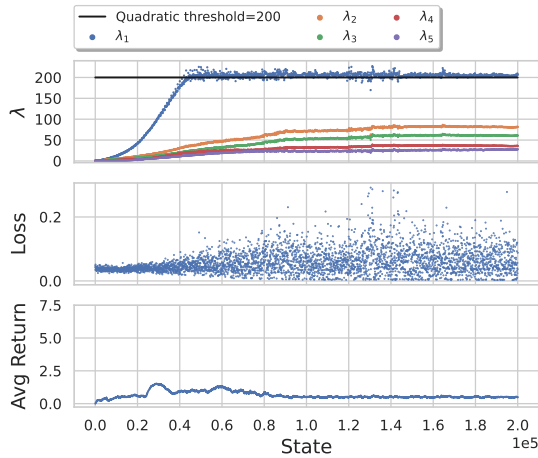


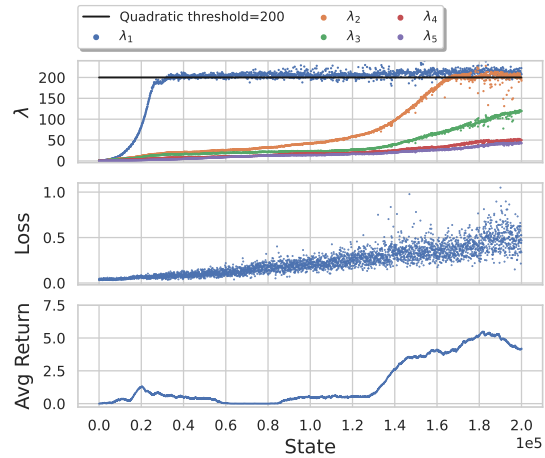
Figure 9: Zoom in full-batch results in the setting Offline RL: agent trained from the replay buffer of a pre-trained agent. **DQN** shows a strong edge of stability effect. The behaviour is consistent with supervised learning where the loss and leading eigenvalue have the same relationship across changes to the target network.

A.3. SGD results for DQN and C51 on Breakout

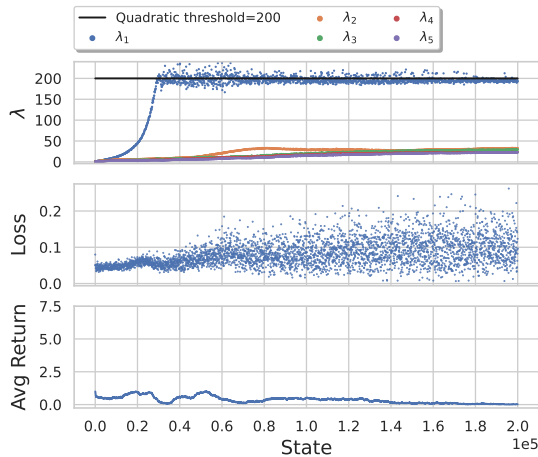
In Figure 10 we present DQN results on Breakout with SGD without momentum which do not clearly show an edge of stability effect. In the online regime, the eigenvalues consistently fail to rise to the quadratic threshold but reach low levels and plateau later in training. There is a clear edge of stability effect offline.



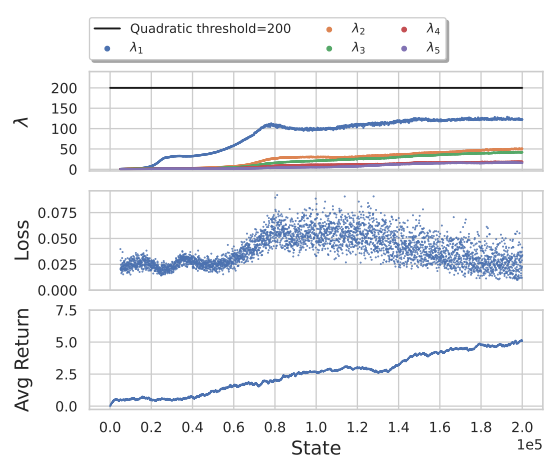
(a) Offline RL: agent trained using experience generated from a greedy pre-trained policy.



(b) Offline RL: agent trained using experience generated from an ϵ -greedy pre-trained policy.



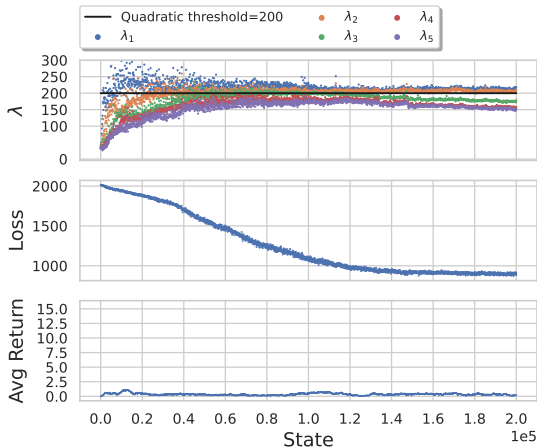
(c) Offline RL: agent trained from the replay buffer of a pre-trained agent.



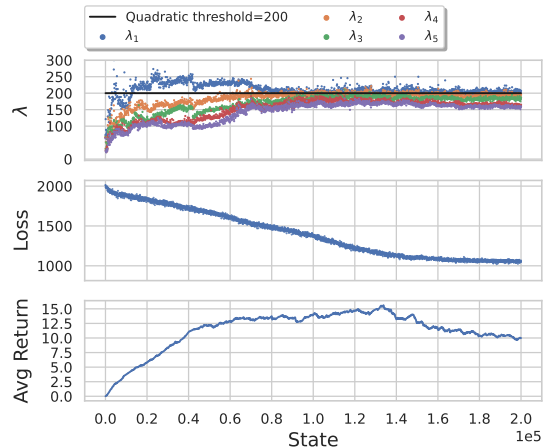
(d) Online RL: agent trained from a replay buffer of its own experience.

Figure 10: **DQN**. The edge of stability phenomenon is observed in the offline setting (10a, 10b and 10c): the leading eigenvalue λ_1 rises to the quadratic threshold, after which it hovers around the quadratic threshold, albeit with some noise; when λ_1 reaches the quadratic divergence threshold, we observe more loss instability, but this does not always get reflected in the agent’s reward. In online training, λ_1 does not reach the quadratic divergence threshold.

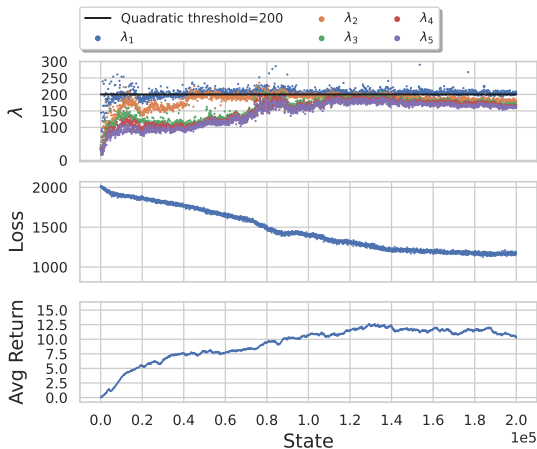
In Figure 11 we present C51 results on Breakout with SGD without momentum which show an edge of stability effect. In the offline regimes, the eigenvalues rise slightly past the quadratic threshold and then decrease to hover around it. In the online regime, the eigenvalues consistently rise orders of magnitude above the quadratic threshold.



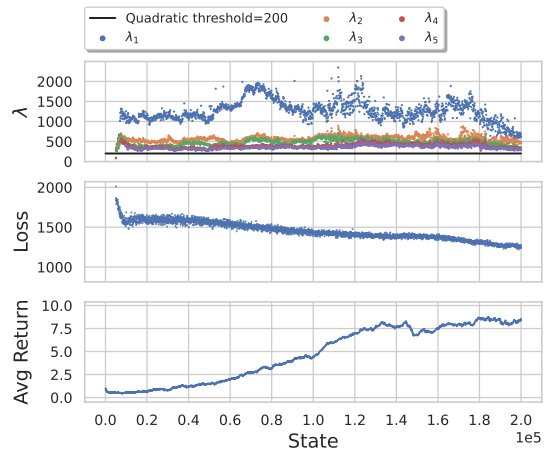
(a) Offline RL: agent trained using experience generated from a greedy pre-trained policy.



(b) Offline RL: agent trained using experience generated from an ϵ -greedy pre-trained policy.



(c) Offline RL: agent trained from the replay buffer of a pre-trained agent.

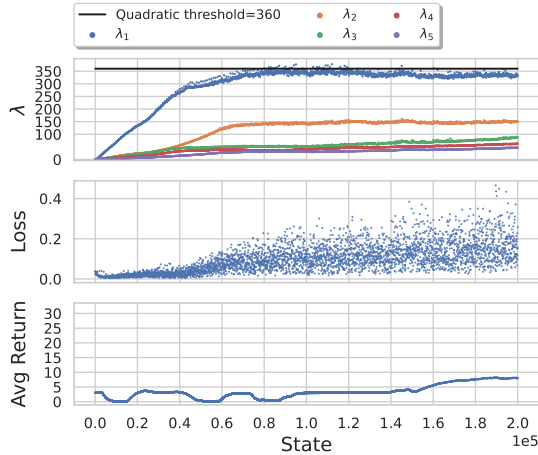


(d) Online RL: agent trained from a replay buffer of its own experience.

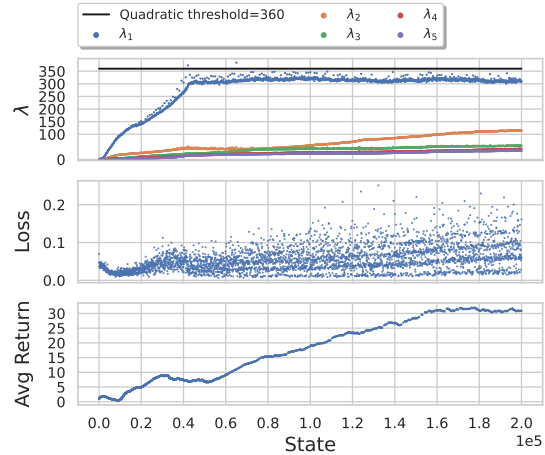
Figure 11: **C51**. When using C51 in an offline setting with SGD, we notice that the leading eigenvalue λ_1 now reaches the edge of stability threshold. In online learning, we observe that λ_1 greatly exceeds the quadratic divergence threshold. Like in supervised learning, however, using a cross entropy loss leads to a decrease of λ_1 later in training.

A.4. Results for DQN in the Space Invaders environment with and without momentum

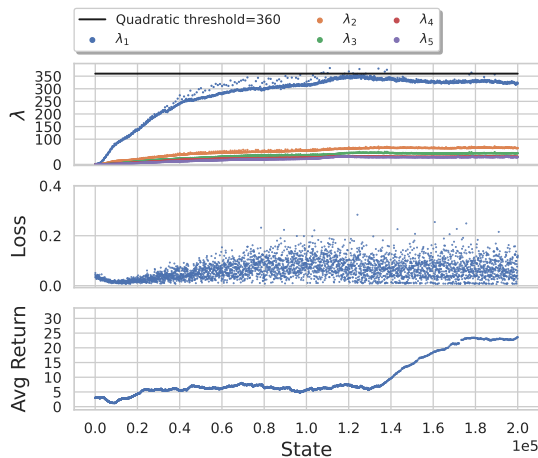
In Figure 12 we present DQN results on Space Invaders with SGD with momentum which clearly show an edge of stability effect in every offline setting. In the online regime, the eigenvalues consistently rise above the quadratic threshold and it has no effect on the trend of the sharpness (λ_1).



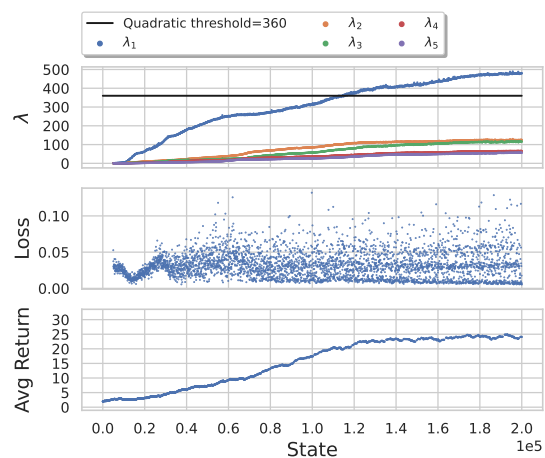
(a) Offline RL: agent trained using experience generated from a greedy pre-trained policy.



(b) Offline RL: agent trained using experience generated from an ϵ -greedy pre-trained policy.



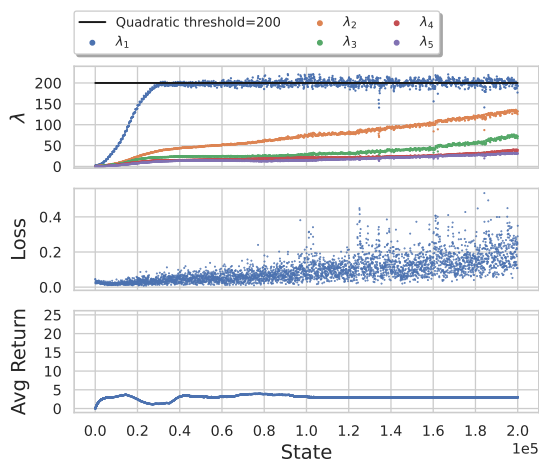
(c) Offline RL: agent trained from the replay buffer of a pre-trained agent.



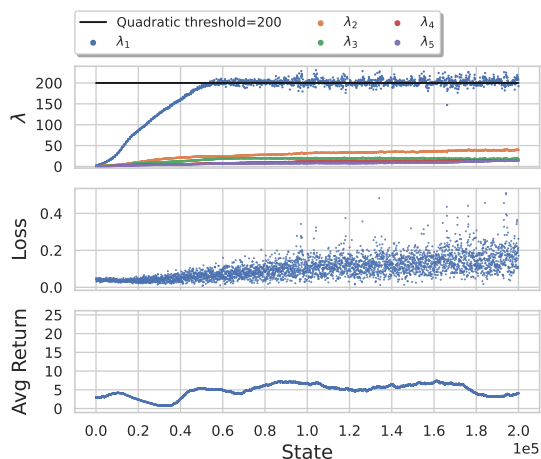
(d) Online RL: agent trained from a replay buffer of its own experience.

Figure 12: **DQN**. The edge of stability phenomenon is observed in the offline setting (12a, 12b and 12c): the leading eigenvalue λ_1 rises to the quadratic threshold, after which it hovers around the quadratic threshold, albeit with some noise; when λ_1 reaches the quadratic divergence threshold, we observe more loss instability, but this does not always get reflected in the agent's reward. In online training, λ_1 exceeds the quadratic divergence threshold. Here SGD with momentum was used.

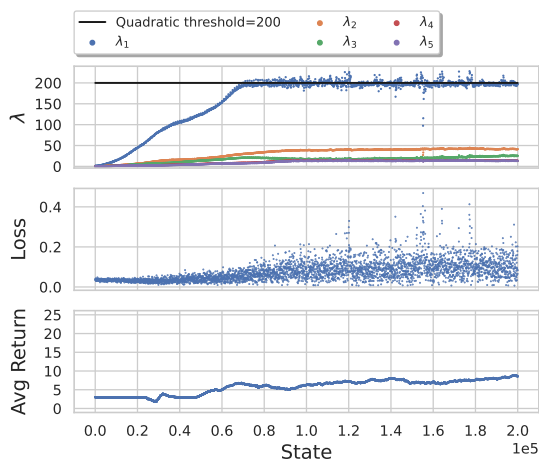
In Figure 13 we present DQN results on Space Invaders with SGD without momentum which clearly show an edge of stability effect in every offline setting. In the online regime, there exists a trace of the edge of stability behaviour, however, later during training the principal eigenvalue consistently rises above the quadratic threshold.



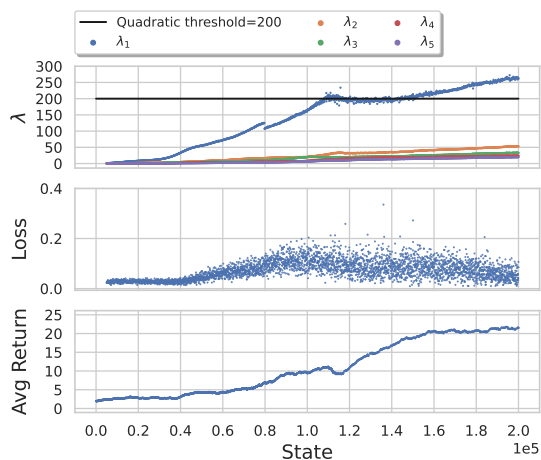
(a) Offline RL: agent trained using experience generated from a greedy pre-trained policy.



(b) Offline RL: agent trained using experience generated from an ϵ -greedy pre-trained policy.



(c) Offline RL: agent trained from the replay buffer of a pre-trained agent.



(d) Online RL: agent trained from a replay buffer of its own experience.

Figure 13: **DQN**. The edge of stability phenomenon is observed in the offline setting (13a, 13b and 13c): the leading eigenvalue λ_1 rises to the quadratic threshold, after which it hovers around the quadratic threshold, albeit with some noise; when λ_1 reaches the quadratic divergence threshold, we observe more loss instability, but this does not always get reflected in the agent's reward. In online training, λ_1 exhibits the edge of stability effect briefly but then it exceeds the quadratic divergence threshold. Here SGD without momentum was used.

Appendix B. Experimental details

B.1. Neural architectures

We used a similar neural network architecture for both DQN and C51. The network consists of 1 Convolutional Layer, followed by 1 Fully Connected (FC) Layer with and an Output Layer which depends on the algorithm. The Convolutional Layer has a kernel size of 3 and a stride of 1 and is configured differently based on the game due to different channel numbers. The rest of the details can be found in Table 1.

Table 1: Parameter settings for the neural network architectures.

Algorithm	Convolutional Layer width	FC Layer width	Output Layer width
DQN	16	128	$num_actions$
C51	16	128	$num_actions \times num_atoms$

B.2. Algorithms

The pseudocode for the DQN algorithm is presented below¹:

Algorithm 1 Deep Q-learning with experience replay

Initialize replay memory D to capacity N

Initialize action-value function Q with random weights θ

Initialize target action-value function \hat{Q} with random weights $\hat{\theta} = \theta$

for $episode=1, \dots, M$ **do**

Initialize sequence $s_1 = \{x_1\}$ and pre-processed state $\phi_1 = \phi(s_1)$ **for** $t = 0, 1, \dots, T$ **do**

With probability ϵ select random action a_t

otherwise select $a_t = \operatorname{argmax}_a Q(\phi(s_t), a; \theta)$

Execute action a_t in emulator and observe reward r_t and image x_{t+1}

Set $s_{t+1} = s_t, a_t, x_{t+1}$ and preprocess $\phi_{t+1} = \phi(s_{t+1})$

Store transition $(\phi_t, a_t, r_t, \phi_{t+1})$

Sample random minibatch of transitions $(\phi_j, a_j, r_j, \phi_{j+1})$

Set $y_j = \begin{cases} r_j, & \text{if episode terminates at step } j + 1 \\ r_j + \gamma \max_{a'} \hat{Q}(\phi_{j+1}, a'; \hat{\theta}), & \text{otherwise} \end{cases}$

Perform gradient step on $\mathcal{L}(y_j, Q(\phi_j, a_j; \theta))$ with respect to the network parameters θ

Every C steps reset $\hat{Q} = Q$

end

end

Output: Optimal $\pi \approx \pi_*$

As an extension of DQN, [3] proposed to look at the entire value distribution dubbed Z instead of considering expectations. Such a view permits the definition of distributional Bellman equations and operators². Z is described discretely by a number $N \in \mathbb{N}$ and $V_{MIN}, V_{MAX} \in \mathbb{R}$, and whose support is the set of atoms $\{z_i = V_{MIN} + i\Delta z : 0 \leq i < N\}$ with $\Delta z = \frac{V_{MAX} - V_{MIN}}{N-1}$. These

1. A detailed description can be found in [23, 24]

2. The Mathematics behind Categorical DQN is expanded in [3].

atoms represent the "canonical returns" of the distribution and each has probability given by a parametric model $\theta : \mathcal{S} \times \mathcal{A} \rightarrow \mathbb{R}^N$:

$$Z_\theta(s, a) = z_i \text{ with probability } p_i(s, a) = \frac{e^{\theta_i(s, a)}}{\sum_j e^{\theta_j(s, a)}} \quad (2)$$

The update is computed via $\hat{\mathcal{T}}Z_\theta$ where $\hat{\mathcal{T}}$ is an operator but a discrete distributional view poses a problem because Z_θ and $\hat{\mathcal{T}}Z_\theta$ almost always have disjoint sets. To combat this issue, the update is reduced to multi-class classification by being projected onto the support of Z_θ . Assume that π is the greedy policy w.r.t $\mathbb{E}[Z_\theta]$. Given a tuple (s, a, r, s', γ) the term $\hat{\mathcal{T}}z_j = r + \gamma z_j$ for each atom z_j . The probability $p_j(s', \pi(s'))$ is distributed to the immediate neighbours of $\hat{\mathcal{T}}z_j$ via a projection operator Φ whose i^{th} component is given by³:

$$\left(\Phi \hat{\mathcal{T}}Z_\theta(s, a)\right)_i = \sum_{j=0}^{N-1} \left[1 - \frac{\left| \left[\hat{\mathcal{T}}z_j \right]_{V_{MIN}}^{V_{MAX}} - z_i \right|}{\Delta z} \right]_0^1 p_j(s', \pi(s')) \quad (3)$$

In the end, as a DQN derivative, a policy network and a target network model Z_θ and $Z_{\hat{\theta}}$ (respecting the notation of Algorithm 1) with the loss \mathcal{L} given by the cross-entropy term of the KL Divergence:

$$D_{KL} \left(\Phi \hat{\mathcal{T}}Z_{\hat{\theta}}(s, a) \parallel Z_\theta(s, a) \right) \quad (4)$$

The routine of Categorical DQN is the same as before with the only expectation being the loss computation which is given by:

Algorithm 2 The Categorical algorithm **Input:** tuple $(s_t, a_t, r_t, s_{t+1}, \gamma_t \in [0, 1])$

$\hat{Q}(\phi_{t+1}, a) := \sum_i z_i p_i(\phi_{t+1}, a)$
 $a^* \leftarrow \operatorname{argmax}_a \hat{Q}(\phi_{t+1}, a)$
 $m_i = 0, i \in \{0, 1, \dots, N-1\}$
for $j = 0, 1, \dots, N-1$ **do**
 $\hat{\mathcal{T}}z_j \leftarrow [r_t + \gamma_t z_j]_{V_{MIN}}^{V_{MAX}}$
 $b_j \leftarrow (\hat{\mathcal{T}}z_j - V_{MIN}) / \Delta z$
 $l \leftarrow \lfloor b_j \rfloor, u \leftarrow \lceil b_j \rceil$
 $m_l \leftarrow m_l + p_j(\phi_{t+1}, a^*)(u - b_j)$
 $m_u \leftarrow m_u + p_j(\phi_{t+1}, a^*)(b_j - l)$

end

Output: $-\sum_i m_i \log p_i(s_t, a_t)$

▷ Cross-entropy loss

B.3. Offline RL reproduction details

In this paper we examined three different offline RL replay buffers for Breakout on Minatar:

3. The quantity $[\cdot]_a^b$ bounds the argument in the interval $[a, b]$.

- 10^6 transitions that were obtained from the experience of a pre-trained agent with no action perturbation.
- 10^6 transitions that were obtained from the experience of a pre-trained agent where during game-play 30% of the actions taken were random (instead of greedy actions being taken).
- 10^6 transitions that were obtained from last 10^6 transitions from the replay buffer of an agent that was trained with Adam, online.

B.4. Optimisation details and how to replicate results

We studied both the full-batch the mini-batch settings of GD and momentum for both algorithms. The mini-batch experiments always used a batch size of 512 and the full-batch experiments were performed on a sub-sample of 10^4 transitions from the original replay buffers which consisted of 10^6 transitions.

When experimenting with gradient descent, the learning rate was 0.01 and when adding momentum the learning rate was 0.01 and the momentum coefficient was $\beta = 0.8$. The initial γ parameter to discount reward was 0.99. The agent which generated the replay buffers was trained with Adam with a batch size of 64, learning rate of 0.00025, $\beta_1 = 0.9$, $\beta_2 = 0.999$ and $\epsilon = 10^{-8}$. Figure 14 shows the return obtained for Breakout online with these settings. During offline training, the action executed by the agent is the action present in the replay buffer. During online training, the first 5000 iterations are used to accumulate experiences in the replay buffer, after which the training of the agent starts. During the first 5000 steps the agent is taking random actions. Afterwards, the actions are taken based on a decaying ϵ -greedy policy where ϵ decreases linearly from 1.0 to 0.1 for 100000 iterations. For C51, we used 51 atoms with $V_{MIN} = -10$ and $V_{MAX} = 10$.

The eigenvalues were logged at every 100 iterations. Whenever "Avg Return" was mentioned, that referred to a moving average of the return per episode. It was calculated based on the following routine: $avg_return[i] = 0.99 * avg_return[i - 1] + 0.01 * return_per_episode[i]$ where $avg_return[0] = return_per_episode[0]$.

The datasets for Breakout and Space Invaders used for experiments are available [here](#). In addition, we are able to provide datasets for performing similar experiments on Asterix, Freeway and Seaquest, the other games present in the Minatar testbed.

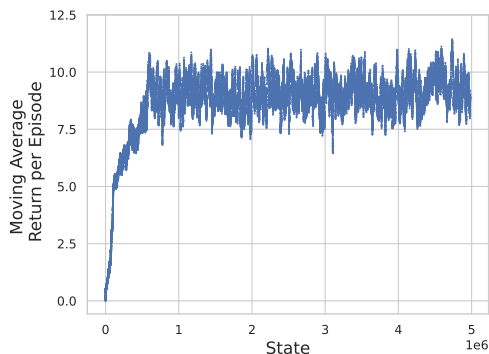


Figure 14: Adam results on Breakout showing the moving average return obtained by the agent during online training.

